FULL PAPER doi.org/10.1002/adsc.202100296 Advanced Synthesis & Catalysis

Semi-Rational Engineering of Toluene Dioxygenase from *Pseudomonas putida* F1 towards Oxyfunctionalization of Bicyclic Aromatics

Julian L. Wissner,[a] Jona T. Schelle,[a] Wendy Escobedo-Hinojosa,[a] Andreas Vogel,[b] and Bernhard Hauer[a,*]

[a] Institute of Technical Biochemistry, University of Stuttgart, Allmandring 31, 70569 Stuttgart, Germany
Tel: +49 711 685–63193;
E-mail: bernhard.hauer@itb.uni-stuttgart.de
[b] c-LEcta GmbH, Perlickstr. 5, 04103 Leipzig, Germany

Manuscript received: March 8, 2021; Revised manuscript received: April 12, 2021;
Version of record online: April 27, 2021

Supporting information for this article is available on the WWW under https://doi.org/10.1002/adsc.202100296

Abstract: Toluene dioxygenase (TDO) from *Pseudomonas putida* F1 was engineered towards the oxyfunctionalization of bicyclic substrates. Single and double mutant libraries addressing 27 different positions, located at the active site and entrance channel were generated. In total, 176 different variants were tested employing the substrates naphthalene, 1,2,3,4-tetrahydroquinoline, and 2-phenylpyridine. Introduced mutations in positions M220, A223 and F366, exhibited major influences in terms of product formation, chemo-, regio- and enantioselectivity. By semi-rational evolution, we lighted up the TDO capability to convert bulkier substrates than its natural substrate, at unprecedented reported conversions. Thus, the most active TDO variants were applied to biocatalytic oxyfunctionalizations of 1,2,3,4-tetrahydroquinoline, and 2-phenylpyridine, enabling the production of substantial amounts of (+)-(*R*)-1,2,3,4-tetrahydroquinoline-4-ol (71% isolated yield, 94% *ee*) and (+)-(1*S*,2*R*)-3-(pyridin-2-yl)cyclohexa-3,5-diene-1,2-diol (60% isolated yield, 98% *ee*), respectively. Here, we provide a set of novel TDO-based biocatalysts useful for the preparation of oxyfunctionalized bicyclic scaffolds, which are valuable to perform downstream synthetic processes.

Keywords: Biocatalysis; Biotransformations; Hydroxylation; Mutagenesis; Rieske non-heme iron dioxygenases

Introduction

The selective oxyfunctionalization of aromatic and heteroaromatic compounds is of great interest for the generation of chiral synthons for pharmaceuticals and fine chemicals.[1–4] Mono- and dihydroxylated aromatics can be obtained by the use of multicomponent Rieske-non heme iron dioxygenases (ROs), which consist of an oxygenase, a reductase and optionally a ferredoxin. ROs are capable to incorporate molecular oxygen into aromatics, creating valuable and chiral *cis*-dihydrodiendiols. Furthermore, this remarkable class of enzymes is capable to perform a variety of different reactions, for instance monohydroxylations, sulfoxidations, desaturations and C-H amination.[5–8] Toluene dioxygenase (TDO) from *Pseudomonas putida* F1, is one of the best studied ROs in the last decades. Its striking promiscuity embraces over 100 non-natural substrates.[9] In terms of catalytic efficiency, TDO is capable of affording astonishingly high titers of monocyclic aromatics, such as bromobenzene, at up to 35 g L^{-1}.[10] Nevertheless, in comparison to naphthalene dioxygenase (NDO), cumene dioxygenase (CDO), and biphenyl dioxygenase (BPDO), from of *Pseudomonas putida* 9816-4, *Pseudomonas fluorescens* IP01, and *S. yanoikuyae* B8/36, respectively, TDO yields lower product formation for bicyclic aromatic substrates. Such reduced performance of TDO in front of bicyclic

aromatics might correlate with the smaller active pocket size, when compared with the ones found in NDO and BPDO.[11] For instance, for the flat bicyclic substrate naphthalene, TDO generates 10 g L^{-1} of the dihydroxylation product, while for the more sterically demanding biphenyl it yields only 3.0 g L^{-1}.[1] Besides, the presence of one nitrogen atom in one of the aromatic rings, results in a drastic decrease in TDO product formation, such as in the case of 2-phenylpyridine (only 1%).[11] This pattern suggests that TDO displays a substrate-size dependent performance (Scheme 1). In order to overcome limitations regarding product formation and selectivity of TDO, previous studies employed directed evolution techniques for generating TDO variants.[12,13] For instance, Zhang and colleagues evolved TDO using random mutagenesis towards the conversion of indene to *cis*-indandiol, a potential key intermediate in the chemical synthesis of the anti-viral Crixivan®.[14] A drawback of directed evolution is the massive screening effort that has to be performed, usually comprising thousands of variants. An attractive and feasible alternative is the rational-design of a reduced set of TDO variants via site-directed mutagenesis. In this case, by employing either bioinformatics tools, such as, *in silico* studies or previous knowledge of experimental data, candidate key positions can be identified and utilized for mutagenesis.[15–17] For instance, Vila and co-workers employed a smartly designed set of TDO active site variants at positions I324, T365 and F366, all three exhibiting major influences in regio- and enantioselectivity.[18] To investigate hot-spot positions

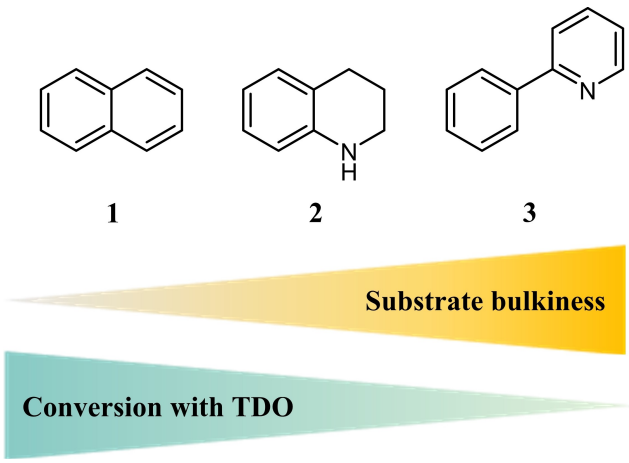

Scheme 1. Substrates employed in this study for the characterization of TDO catalyzed hydroxylation patterns. Naphthalene **1**, 1,2,3,4-tetrahydroquinoline **2**, and 2-phenylpyridine **3**. Substrate bulkiness (yellow gradient), increases from left **1** to right **3**. Substrate conversion displayed by TDO wild type (green gradient), shows an inverse correlation with respect to the substrate bulkiness from left **1** (high conversion) to right **3** (low conversion).

influencing the conversion of bicyclic aromatics, we designed a set of semi-rational TDO variants, which were generated via site-directed mutagenesis by c-LEcta (Leipzig, DE). Our approach resulted in the identification of engineered TDO variants displaying remarkable conversion activities towards all tested bicyclic aromatics. Findings reported herein foster the biocatalytic synthesis of valuable oxyfunctionalized aromatic bicyclic scaffolds.

Results and Discussion

To our best knowledge, a detailed study on the influence of the TDO active site residues, driving product formation, chemo-, regio- and stereoselectivity was so far, not performed. In order to foster the TDO catalyzed conversion of bicyclic aromatic substrates, we employed site-directed mutagenesis aiming to engineering; 1) the active site, 2) the putative substrate entrance channel, and 3) literature known key positions of the TDO system (supplementary section 3).

1) For the generation of active site variants, we used the 3DM database of Bio-Prodict (Nijmegen, NL), to align the sequences of 671 ROs of the toluene/benzene, naphthalene, and cumene dioxygenase sub-families. All active site positions[15,19] with a conservation below 90% were chosen for mutagenesis (Q215, F216, M220, A223, G264, Y266, L272, I276, V309, H311, L321, I324, F366 and F372). The highly conserved position H222, H228 and D376, coordinating the catalytic iron, as well as D219 were therefore not considered. The 14 active site positions were mutated into amino acids, which exhibited according to the sequence alignment, an occurrence of over 2% (Table S2).

2) The substrate channel was modelled using the crystal structure of the TDO α-subunit (PDB ID; 3EN1) and the CAVER plugin (version 3.0.1) for PyMOL (supplementary section 6). To investigate the influence of the substrate channel size, all amino acids around 5 Å of the putative substrate channel (G224, T225, L229, L245, P247 and P248) were replaced by an alanine (Table S3).

3) At last, seven positions, either previously described in literature or suggested by the 3DM database as hot-spot position (F114, T115, A212, A234, G323, V340, T365), were chosen for mutagenesis.[14,18,20,21]

Thus, a total of 121 single variants at 27 different amino acid positions were generated (Table S1) and investigated towards the bicyclic substrates; naphthalene **1**, 1,2,3,4-tetrahydroquinoline **2**, and 2-phenylpyridine **3** (Scheme 1). Lastly, since the screening of the mutant library with substrates **1**–**3** highlighted variants at positions M220 and A223 as beneficial for an increased product formation, we selected such positions to generate a second mutant

library consisting out of 55 double variants focused on positions M220 and A223 (Table S4). Consequently, we describe in the current study 176 semi-rational designed single and double variants (Table S1 and S4). In addition to the characterization of these variants, we aimed for the semi-preparative production of the identified products, employing the outperforming engineered TDO variants (Scheme 2).

Screening of the mutant library was performed according to experimental section 1.3. Variants fulfilling one or more of the following criteria were validated according to experimental section 1.4 as follows; 1) Variants displaying over 200% total product formation in comparison with the TDO wild type, 2) Variants showing a switch in product distribution in favor to the side product, and in addition, at least 50% total product formation, when compared to TDO wild type, 3) Variants generating selectively one product, 4) Double variants have to be at least as active or as selective as the parent single variant. In addition, the enantiomeric excess for **1a**, **2a**, and **3a** was determined via chiral HPLC-DAD for the validated variants (experimental section 1.9).

The screening of the single mutant library with substrate **1**, highlighted the active site positions M220 and A223 boosting the formation of **1a** (Figure S25). Validation of the single point variants M220A, A223I and A223V showed a 2.6-, 2.3-, and 5.0-fold increase in product formation, in comparison with TDO wild type, respectively (Table 1). The enantiomeric excess for **1a** (>98%), remained the same for all three variants. Double variants at the positions M220 and A223 were not able to surpass the product formation of their corresponding single point parent variants. Thus, for **1a** the highest product formation of 6.27±0.08 mM (62.7%) was achieved with the variant A223V, employing 10 mM substrate, within only 0.5 h, clearly illustrating the feasibility of engineering TDO towards bicyclic aromatics. As previously reported, active site variant F366V exhibited a switch from >98% *ee* **1a** to −90, while decreasing, in comparison to the TDO wild type, 20.8-fold the product formation.[17] Such dramatic reduction in naphthalene conversion with TDO_{F366V} compared to the fast occurring TDO wild type driven reaction, can be explained by the short established reaction time (only 0.5 h) and the restrictive working conditions, in terms of air to liquid ratio, to perform the biotransformations. Double variants TDO_{F216A_F366V} and TDO_{M220A_F366V} showed nor a further improvement in enantioselectivity (−70% *ee* and 13% *ee*, respectively), neither an increased product formation, compared to the single point variant TDO_{F366V} (data not shown).

TDO wild type showed an initial acceptance for substrate **2**, yielding products **2a** and **2b** after 20 h of biotransformation employing 10 mM of **2**. The monohydroxylated compound **2a** was the main product (2.74±0.18 mM, 77% *ee*), while the dehydrogenated compound **2b** was secondary (0.22±0.02 mM). As expected, the observed conversion for **2** (only 30%) was lower in comparison to **1** (100%), due to the larger size of substrate **2**. It is worth to mention that product **2a** is of great interest, considering its relevance as pharmaceutical synthon.[22–24] Thus, fostering **2a** production became an enticing task for this work. By testing the single point TDO library with substrate **2** we identify the active site positions A223 and L321, and position F114, located at the putative ferredoxin binding site,[20] as positive hits favoring the total product formation (Figure S26). Validation of the variants F114H and A223V indicated a 1.9- and 1.7-fold increase in total product formation, respectively,

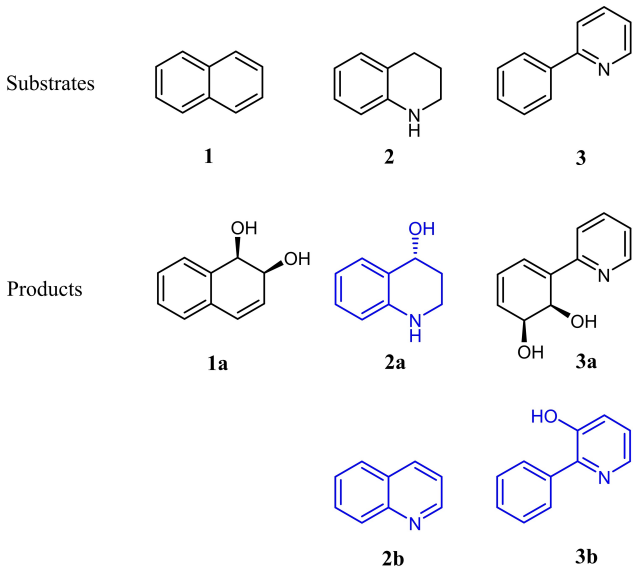

Scheme 2. TDO wild type catalyzed conversion of the substrates naphthalene **1**, 1,2,3,4-tetrahydroquinoline **2**, and 2-phenylpyridine **3**. Generated products; (+)-(1*R*,2*S*)-1,2-dihydro-1,2-naphthalenediol **1a**, (+)-(*R*)-1,2,3,4-tetrahydroquinoline-4-ol **2a**, quinoline **2b**, (+)-(1*S*,2*R*)-3-(pyridin-2-yl)cyclohexa-3,5-diene-1,2-diol **3a**, and 2-phenylpyridin-3-ol **3b**. Novel products identified in this work, **2a**, **2b**, and **3b**, are depicted in blue.

Table 1. Validation of variants with increased product formation and/or switched product distribution for naphthalene **1** (10 mM).

Variant	PF of **1a** [mM][a]	*ee* of **1a** [%][b]
WT	1.25±0.04	>98
M220A	3.28±0.24	>98
A223I	2.85±0.69	>98
A223V	6.27±0.08	>98
F366V	0.06±0.03	−90

[a] PF stands for product formation.
[b] *ee* stands for enantiomeric excess.

and maintained the same product distribution (**2a**:**2b**; 92:8), as for the TDO wild type driven reaction (Table 2). Active site variant A223T was not only capable of converting the total amount of substrate **2** (10 mM), but also favored the synthesis of the interesting product **2a** (**2b** concentration remained <0.04 mM). Variant L321A also increased the total product formation 1.9-fold, however, the exhibited product distribution was altered (**2a**:**2b**; 72:28). In contrast, active site variants M220A, L321S and F366V showed a switch in chemoselectivity, favoring now the generation of the secondary product **2b**. The observed distributions **2a**:**2b** were as follows; 28:72, 17:83 and, 26:74, for variants M220A, L321S, and F366V, respectively. Along with the chemoselectivity switch, a decreased total product formation was observed in comparison with TDO wild type, resulting in a reduction of 3.3-, 2.4-, and 3.1-fold, for mutants M220A, L321S, and F366V, respectively. Double variant TDO_{F114H_A223T} surpassed the beneficial chemoselectivity of the single variant TDO_{A223T}, since full conversion was achieved, and product formation was exclusively directed toward **2a** formation. In addition, the combinatorial double variant F114H_A223T exhibited higher enantiomeric excess (83% *ee*), compared to the wild type and the corresponding single parent variants F114H and A223T (for both cases, 77% *ee*). Thus, the double variant not only outperformed TDO wild type, but also all tested variants, enabling the selective production of 9.93 ± 0.24 mM (99.3%) of **2a** with 83% *ee*. Interestingly, all single and double variants containing amino acid exchanges at position M220, exhibited, compared to TDO wild type, a decreased product formation along with an altered chemoselectivity. We managed to foster the enantiomeric excess in favor to **2a** by altering the pH value of the reaction buffer (supplementary section 5). Thus, at higher pH-value the enantiomeric excess for **2a** was increased. Such effect might be explained by the racemization of **2a** at acidic conditions.[25] As a result, biotransformations performed in 0.1 M TRIS-buffer pH 8.5 exhibited an *ee* of 97 and 95%, for TDO wild type and for TDO_{F114H_A223T}, respectively. Moreover, the **2a**:**2b** product ratio remained the same as observed for the biotransformations performed in 0.1 M potassium phosphate buffer pH 7.4 (Table S8). An increased total product formation (4.13 ± 0.46 mM) was obtained in the case of TDO wild type driven reactions employing TRIS-buffer pH 8.5. However, the opposite effect was observed for TDO_{F114H_A223T}, resulting in a product reduction down to 8.58 ± 0.18 mM, instead of the 9.93 ± 0.24 mM generated product observed in potassium phosphate buffer pH 7.4. Among all tested variants, TDO_{F366V} showed the highest total product formation favoring **2b** (2.79 ± 0.11 mM, **2a**:**2b**; 27:73), in biotransformations performed in TRIS-buffer pH 8.5. Besides, altering TRIS-buffer pH to 9.0, led to even higher *ee* values for **2a**, but at the expense of total product formation (data not shown). For a conclusive product identification and structural characterization, semi-preparative biotransformations in 0.1 M TRIS-buffer pH 8.5 were performed, employing the selected variants TDO_{F114H_A223T} and TDO_{F366V}, for the generation of **2a** and for **2b**, respectively. Semi-preparative biotransformation of **2** with TDO_{F114H_A223T} yielded 106 mg (71%, 94% *ee*) of **2a** as sole product, while TDO_{F366V} yielded 20 mg (16%) of **2b** and minor amounts of **2a** (<5 mg; not isolated).

Table 2. Validation of variants with increased product formation and/or switched product distribution for 1,2,3,4-tetrahydroquinoline **2** (10 mM) at pH 7.4 (0.1 M potassium phosphate buffer).

Variant	PF of **2a** [mM][a]	PF of **2b** [mM][a]	*ee* of **2a** [%][b]
WT	2.74 ± 0.18	0.22 ± 0.02	77
F114H	5.07 ± 0.40	0.44 ± 0.04	77
M220A	0.25 ± 0.01	0.64 ± 0.02	60
A223T	9.91 ± 0.21	0.04 ± 0.01	77
A223V	4.61 ± 0.17	0.49 ± 0.02	78
L321A	3.96 ± 0.20	1.55 ± 0.07	70
L321S	0.21 ± 0.04	1.03 ± 0.09	69
F366V	0.25 ± 0.01	0.73 ± 0.04	83
F114H_A223T	9.93 ± 0.24	0.01 ± 0.01	83

[a] PF stands for product formation.
[b] *ee* stands for enantiomeric excess.

In agreement with literature, conversion of 2-phenylpyridine **3** with TDO wild type yielded **3a** as main product, in slight amounts (0.50 mM, 5%).[11] Such TDO conversion behavior confirmed the trend illustrated in Scheme 1, showing an inverse correlation in terms of substrate size and achieved conversion. Naturally, not only the bulkiness, but also the electronic properties of the substrates can play a role, especially for electron-poor heteroaromatics. Strikingly, TDO conversion of **3** generated, in addition to compound **3a**, the secondary product **3b** (0.11 mM, 1%), a chemical entity not previously reported in the literature. The discovery of **3b** turned out to be of great interest, since the enzymatic hydroxylation of a heteroaromatic moiety in a molecule, connected to an aromatic system, was so far not observed.[11] Electron-poor heteroaromatics, for instance pyridine, are much more resistant to RO catalyzed hydroxylation, than aromatics.[26] Usually, RO catalyzed monohydroxylation of alkyl groups attached to heteroaromatics and *cis*-dihydroxylation of fused aromatics, occur both more readily than the hydroxylation of heteroaromatics. The formation of the monohydroxylated product **3b** involves most likely an unstable *cis*-dihydrodiendiol which undergoes spontaneous dehydration as described for the TDO catalyzed hydroxylation of 4-

picoline to 3-hydroxy-4-picoline.[12] Such novel finding of **3b**, encouraged us to boost its production. Therefore, we investigate whether one of our generated variants was capable to favor **3b** product formation to achieve its substantial synthesis.

The screening of the single point mutant library with substrate **3** highlighted the active site positions M220, A223 and V309 as beneficial for increasing the total product formation (Figure S27). In comparison to TDO wild type, validation of variants M220A, M220C, A223I, A223V and V309G showed a 12.4-, 8.5-, 6.5-, 6.4-, and 9.4-fold increase in the total product formation, respectively (Table 3). However, among all the positive hits, only variant M220A maintained the product ratio (**3a**:**3b**; 82:18), observed in TDO wild type, whereas variants A223I and A223V favored the production of **3a** (**3a**:**3b**; 91:9 and 86:14, respectively). In contrast, variant M220C exhibited an increase in product formation for **3b**, by altering the product distribution (**3a**:**3b**; 64:36). Thought variants F216 A and F366V, compared to the wild type, exhibited a decreased total product formation (4.4- and 8.7-fold, respectively), both were capable to astoundingly switch the product ratio in favor to **3b** (**3a**:**3b**; 12:88 and 0:100, respectively). Despite we focused our attention on the **3b** entity, we were also interested in following the library performance toward **3a** synthesis. In this way, we found a strong improvement in **3a** product formation by employing the combinatorial double variants TDO_{M220A_A223V} and TDO_{M220A_V309G}. Both combinations led to an impressive 14.0- and 15.1-fold increase in total product formation, compared to the wild type, both favoring the production of the *cis*-dihydrodiendiol **3a** (**3a**:**3b**; 92:8 and 93:7, respectively). Product formation increase might be correlated with the enlargement of the active pocket, for variant TDO_{M220A_V309G} (Figure S31). Regarding the enantiomeric excess for product **3a**, no alterations were detected since all tested variants showed an *ee* >98%. For practical purposes and a viable production of substantial amounts of both **3a** and **3b**, we selected TDO_{M220A_V309G} to perform a semi-preparative biotransformation. This approach enabled the formation of 8.51 ± 0.31 mM (85.1%) **3a** and 0.64 ± 0.03 mM (6.4%) **3b**, resulting in a conversion of 91.5%, which is impressive considering that the starting performance of TDO wild type was as low as 6.1%. In terms of isolated product yield, this translates in 114 mg (60%; *ee* >98%) and 6 mg (4%) for **3a** and **3b**, respectively.

Table 3. Validation of variants with increased product formation and/or switched product distribution for 2-phenylpyridine **3** (10 mM).

Variant	PF of **3a** [mM][a]	PF of **3b** [mM][a]	*ee* of **3a** [%][b]
WT	0.50 ± 0.08	0.11 ± 0.02	>98
F216A	0.02 ± 0.01	0.13 ± 0.02	n.d.
M220A	6.26 ± 0.13	1.32 ± 0.06	>98
M220C	3.32 ± 0.21	1.89 ± 0.16	>98
A223I	3.62 ± 0.28	0.37 ± 0.03	>98
A223V	3.36 ± 0.46	0.54 ± 0.08	>98
V309G	5.50 ± 0.40	0.24 ± 0.01	>98
F366V	0.00 ± 0.00	0.07 ± 0.01	n.d.
M220A_A223V	7.87 ± 0.12	0.64 ± 0.15	>98
M220A_V309G	8.51 ± 0.31	0.64 ± 0.03	>98

[a] PF stands for product formation.
[b] *ee* stands for enantiomeric excess.

We identified semi-rational engineered TDO variants, showing enhanced product formation and selectivity towards bulkier bicyclic aromatic compounds in comparison to the already well accepted substrate naphthalene (Scheme 3).[17] TDO_{F114H_A223T} and TDO_{M220A_V309G} enabled **2** and **3** conversion up to 100 and 91.5% respectively, employing 10 mM of substrate, in comparison with the starting point 29.6 and 6.1%, for TDO wild type. These two variants enabled the production and isolation of the highly valuable compounds **2a** and **3a** with remarkable isolated yields (71% and 60%, respectively), advantageous product selectivity (**2a**:**2b**; 100:0, **3a**:**3b**; 93:7), and outstanding enantiomeric excess (94% and >98% *ee*, respectively). The seven TDO positions, influencing either chemo-, regio- or enantioselectivity, as well as the product formation are summarized in Table 4. All of these positions, except F114, are located in the active site of the TDO (Figure S29).[15,19] Position F114 (corresponding to F99 in NDO from *Pseudomonas sp.* NCIB 9816-4) is located at the ferredoxin binding site, near the Rieske center.[20] Alteration of positions M220, A223 and F366 had a positive impact in terms of chemo-, regio-, enantioselectivity or product formation, for all three tested substrates.

Table 4. TDO positions with major influence on chemo-, regio- and enantioselectivity and positions exhibiting, in comparison to the wild type, an increased product formation for substrates; naphthalene **1**, 1,2,3,4-tetrahydroquinoline **2**, and 2-phenylpyridine **3**.

	TDO positions with major influence on:			
Substrate	Chemoselectivity	Regioselectivity	Enantioselectivity	Product formation
1	–	–	F366	M220, A223
2	M220, A223, L321, F366	–	–	F114, A223, L321
3	–	F216, M220, V309, F366	–	M220, A223, V309

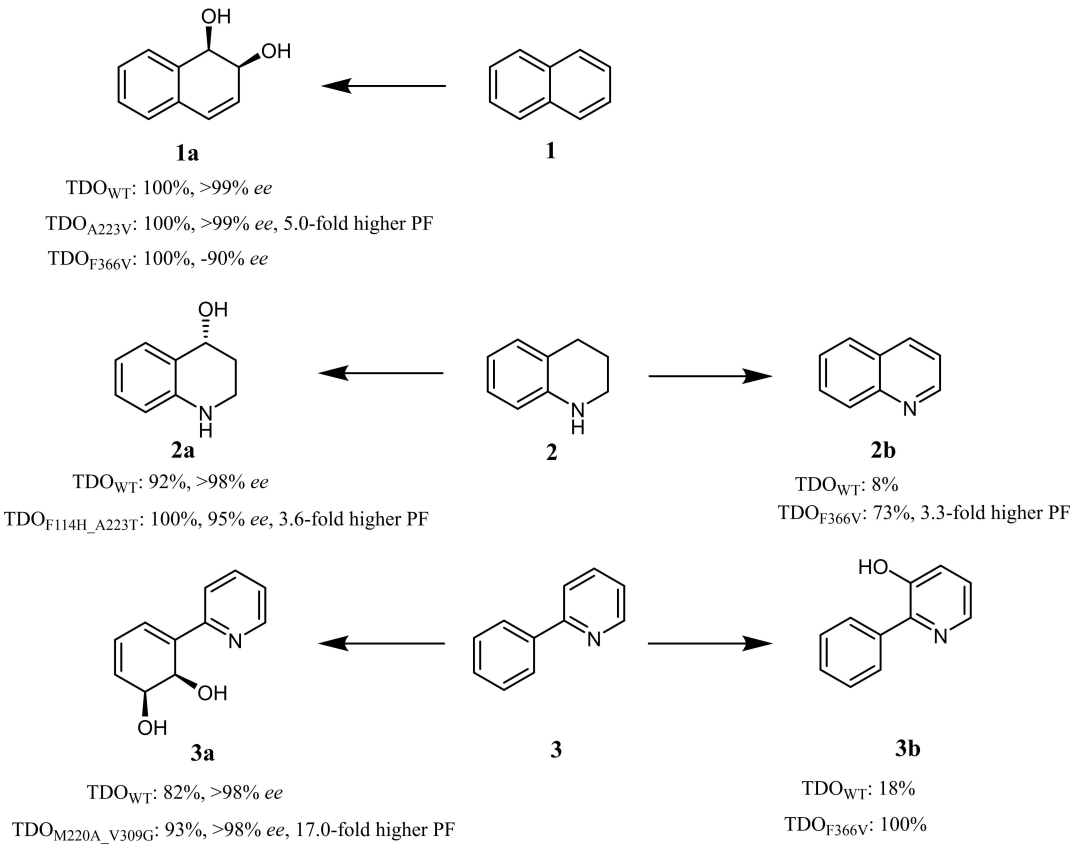

Scheme 3. TDO wild type (TDO$_{WT}$) and identified TDO variants showing enhanced product formation and selectivity, towards the bicyclic substrates **1**, **2** and **3**. Product selectivity (in %) and enantiomeric excess (where suitable, in %), for the wild type and the best variants, is depicted below the generated products for each tested substrate. Higher increase in product formation (PF) for outperforming variants is given in −fold terms, in comparison to the wild type.

Variants at active site position TDO M220, exhibited quite diverse properties regarding the converted substrate. For instance, for substrates **1** and **3**, M220 variants increased the total product formation. Moreover, in the case of **3**, introduced changes also exerted an influence in terms of regioselectivity. All tested M220 variants exhibited an alteration in chemoselectivity for substrate **2**, which mostly favored **2b** production, highlighting the impact of this position. Influence of TDO M220 position on product formation and selectivity has been described in literature, reporting that variant TDO$_{M220A}$ enabled activity towards 1,2,4,5-tetrachlorobenzene, which was not observed with TDO wild type.[27] Relevance of position M220 was also reported for homolog dioxygenase systems such as NDO and CDO, from *Pseudomonas sp.* NCIB 9816-4 and *Pseudomonas fluorescens* IP01, respectively. For NDO, the exchange of alanine to valine at the equivalent position A206 showed substantial influence on product formation, chemo-, regio- and stereoselectivity for substrates ethylbenzene, α-methylstyrene, and allylbenzene.[28] Whereas for CDO, an exchange of methionine to alanine at the corresponding position M232 enabled, for the first time, the conversion of (+)-α-pinene and also exhibited for a variety of substrates, a positive influence in product formation, regio- and enantioselectivity.[29] In this work, for TDO position M220, the exchange to the small amino acids alanine and cysteine led to an increase in product formation for substrates **1** and **3**. The favorable effect of the introduced changes suggest that it could be correlated with the enlargement of the active pocket.

TDO variants addressing position A223 led to an increase in product formation for all three tested substrates. In the particular case of **2**, variants at position A223 exhibited an influence in chemoselectivity. For **3**, the exchange into the small amino acids valine and threonine, as well as to the aliphatic amino acid isoleucine fostered product formation, resulting in a conversion rise up to 6.5-fold. This is the first time that the mentioned catalytic advantages of TDO variants at position A223 are reported. Besides, despite the beneficial role of this position, it has been not described for any of the related TDO homologs and their equivalent positions, such as NDO from *Pseudo-*

monas sp. NCIB 9816-4 (position V209), BPDO from *Pseudomonas pseudoalcaligenes* KF707 (position A234), or CDO from *Pseudomonas fluorescens* IP01 (position A235). The only data available addressing equivalent TDO position A223 was reported for aniline dioxygenase (ADO) from *Acinetobacter sp.* strain YAA. In this case, the exchange into an alanine of the corresponding position V205 in ADO, induced two different effects; on one hand a novel activity, enabling the conversion of 2-isopropylaniline, and on the other hand, a severe conversion decrease for substrates aniline and 2,4-dimethylaniline.[30] Thus, our approach allowed the identification of TDO position A223 as a novel hot spot location strongly influencing product formation.

TDO position F366 showed perhaps, the most versatile influence. Particularly, variant F366V is of great interest, since in reference to the wild type this exchange prompted three different effects; 1) a complete switch in enantioselectivity for **1a** (from >98% to −90% *ee*), 2) a switch in chemoselectivity towards **2b** (from 92:8 **2a**:**2b** to 27:73), and 3) a complete switch in regioselectivity towards **3b** (from 82:18 **3a**:**3b** to 0:100). However, compared to the wild type, all variants at position F366 exhibited a reduced product formation. The influence on enantioselectivity of position TDO F366 was described for naphthalene,[17] bromobenzene, styrene and indene.[18] In the case of the later, in addition to the enantioselectivity influence an alteration in regioselectivity was also observed. Variants at the corresponding position in NDO from *Pseudomonas sp.* NCIB 9816-4 (position F352), exhibited alterations in terms of enantioselectivity for naphthalene, biphenyl, and phenanthrene and also in regioselectivity for the former and the later.[31,32] BPDO variants from *Pseudomonas pseudoalcaligenes* KF707 at the corresponding position (F377) showed altered chemo- and regioselectivity for various chlorinated biphenyls.[33] Taking into account all the reports, it seems that the conserved phenylalanine at position 366 in TDO is not only critical to direct product enantioselectivity in this dioxygenase system, but also in the homologue enzymes NDO and BPDO.

Favorably, for **3**, the bulkier substrate, product formation and product distribution were both enhanced by generating engineered variants which were designed based on a combinatorial approach of the best performing single variants. This approach fostered beyond the observed activity for the single point variants which were already improved in comparison with TDO wild type, for instance, in the case of TDO_{M220A_V309G} driven conversion of **3**. Interestingly, despite of the enlargement generated by exchanging the amino acids located at the putative substrate entrance channel into alanine (Table S3, Figure S30), no beneficial effects were observed.

Conclusion

In the present study we identified a total of seven positions in TDO, critically influencing the oxyfunctionalization of substrates **1**, **2**, and **3**. Furthermore, the hot spot positions M220, A223, and F366 exhibited for all of three tested substrates substantial changes in product formation and in chemo-, regio- and enantioselectivity. Single and double TDO variants at these positions enabled a conversion over 91% out of 10 mM of **2** and **3**. Conversion achievements for **2** and **3** are outstanding, considering that both substrates were initially poorly converted by the wild type enzyme. In addition, semi-preparative biotransformations employing outperforming variants enabled the TDO catalyzed synthesis of products **2a**, **2b**, **3a**, and **3b**, for the first time, in substantial amounts. In conclusion, the semi-rational engineering of TDO indeed endowed a viable oxyfunctionalization towards bulky bicyclic aromatics, in terms of product formation, chemo-, regio- and stereoselectivity.

Experimental Section

Materials. Chemicals and solvents used in this work were obtained at the highest purity degree available from Sigma-Aldrich (St. Louis, US) and Carl Roth (Karlsruhe, DE). 2-Phenylpyridin-3-ol **3b** was purchased at Fluorochem (Hadfield, UK). Substances **2a**, **2b**, **3a**, and **3b** were biosynthesized according to the details given in 1.5.

Bacterial strain, plasmid harboring toluene dioxygenase and mutant library. All biotransformations were performed in a recombinant *E. coli* strain BW25113 harboring the multicomponent toluene dioxygenase (BW25113 pBAD18-TDO), as previously reported.[34] A number of 176 single- and double variants of the TDO α-subunit were generated by c-LEcta (Leipzig, DE). The pBAD18-TDO plasmid, harboring the TDO wild type, was used as template and variants were generated following an oligo-based mutagenesis protocol and verified by Sanger sequencing.

TDO mutant library screening. TDO mutant libraries consist of pBAD18-TDO variants harbored in recombinant *E. coli* BW25113 cells, which were received in the form of glycerol stocks from c-LEcta (Leipzig, DE). Libraries were constantly stored at −80 °C. Cells were reactivated in 96 deep well plates by inoculating 2 µL of the glycerol stocks in 0.5 mL of LB medium supplemented with ampicillin (100 mg L^{-1}). Plates were covered with Breathe-EASIER sealing membranes (Sigma, St. Louis, US) and incubated overnight at 37 °C and 800 rpm in a microplate shaker (VWR International, Radnor, US). Each overnight culture (25 µL) was transferred into a new 96 deep well plate containing, per well, 1.0 mL of TB medium supplemented with ampicillin (100 mg L^{-1}) and were incubated for 2 h at 37 °C and 800 rpm. Subsequently, protein production was induced by addition of L-arabinose to a final concentration of 10 mM, and plates were incubated at 25 °C at 800 rpm for 20 h. Afterwards, cells were harvested by centrifugation at 4000 × *g* at 4 °C for 20 min and the supernatant was discarded.

Cell pellets were resuspended in 0.1 M potassium phosphate buffer (0.49 mL, pH 7.4) supplemented with 20 mM glucose monohydrate and transferred into 96 deep well plates furnished with glass Hirschmann vials (Hirschmann Laborgeräte GmbH & Co. KG, Eberstadt, DE), enabling reusability of 96 deep well plates without cross contamination. Reactions were started by addition of 10 µL of a 0.5 M substrate solution prepared in ethanol, to a final concentration of 10 mM. Biotransformations were incubated at 30 °C and 800 rpm, in the case of substrate naphthalene **1**, only for 0.5 h and in the case of substrates 1,2,3,4-tetrahydroquinoline **2** and 2-phenylpyridine **3** for 20 h. Reactions were stopped by addition of 0.5 mL of the extraction solvent MTBE. After vigorous mixing and centrifugation (4000 × *g* at room temperature for 5 min) the organic layer was removed and analyzed via HPLC-DAD, to quantify the achieved product formation and selectivity. In addition, HPLC-ESI-MS analysis was performed to confirm the masses of the generated products. The whole set of screening results is shown in supplementary section 4, Figures S25–S27.

Validation of mutant library hits. Variants fulfilling one or more of the following criteria were reevaluated with the corresponding substrate: 1) Variants displaying over 200% total product formation in comparison with TDO wild type, 2) Variants showing a switch in product distribution in favor to the side product, and in addition, at least 50% total product formation, when compared to TDO wild type, 3) Variants generating selectively one product, 4) Double variants have to be at least as active or as selective as the parent single variant and fulfill at least one of the criteria previously mentioned.

Biotransformations were performed according to 1.3, with the only difference, that no glass Hirschmann inlets were used. This increased the total working volume from 1.0 mL to 2.0 mL, resulting in an increased product formation for all tested substrates. In addition, the enantiomeric excess of the generated products was determined via chiral HPLC-DAD. Validation results of variants fulfilling the established criteria are shown in Table 1, 2 and 3.

Semi-preparative biotransformations. Semi-preparative biotransformations were performed according to 1.4 with the only exception that for substrate 1,2,3,4-tetrahydroquinoline **2**, the TDO_{F114H_A223T} and TDO_{F366V} catalyzed biotransformations were performed in TRIS-buffer (0.1 M, pH 8.5) supplemented with 20 mM glucose monohydrate instead of potassium phosphate buffer (see supplementary section 5). For semi-preparative biotransformation of **3**, TDO_{M220A_V309G} was employed. A number of 200 simultaneous driven biotransformations were performed in 96 deep well plates, and combined after reaction completion, thus representing a total of 100 mL reaction volume. The combined reaction mixtures were extracted with MTBE either five times (1:1) for **2**, or nine times (1:2) for **3**. The combined organic layers were evaporated *in vacuo* and redissolved in 6 mL of an acetonitrile-water mixture. The purification step was performed by preparative HPLC in an Agilent 1260 Infinity HPLC-DAD system (Santa Clara, US), equipped with a preparative C18-column (Supelco, Discovery C18, 5 µm, 21.2 × 100 mm, Bellefonte, US) and a fraction collector (Agilent 1260 Infinity II, Santa Clara, US). Product purification was performed with a flow rate of 4.0 mL min^{-1} and repeated injections of 70 µL of the crude reaction mixture. The mobile phase for the purification of generated products from substrates **2** and **3** was water/acetonitrile (55/45), which was hold isocratically for 22 min. Peaks were detected at 210 nm for the reaction analysis of **2** and at 310 nm for **3** (Supplementary section 1, Figs. S6 and S13). The collected fractions of each product were evaporated *in vacuo* and analyzed via ^{1}H- and ^{13}C-NMR (supplementary section 2, Figs. S14–S24).

Chemical synthesis of (-)-(*S*)-1,2,3,4-Tetrahydroquinoline-4-ol. The chemical synthesis of (−)-(*S*)-1,2,3,4-tetrahydroquinoline-4-ol was done according to Kolcsar and collegues.[35] The raw product was extracted five times with MTBE, evaporated *in vacuo* and dissolved in 4 mL ACN. Preparative HPLC purification was performed as described in 1.5. A total of 28.1 mg (10% yield) (−)-(*S*)-1,2,3,4-tetrahydroquinoline-4-ol was obtained. The enantiomeric excess for raw and purified product was determined via chiral HPLC-DAD to 81% *ee* and 35% *ee*, respectively.

HPLC-DAD for quantification. For substrate **1** biotransformations HPLC-DAD and ESI-MS methods were performed according to Wissner and colleagues.[17] For the analysis of the biotransformation products of substrates **2** and **3**, an Agilent 1260 Infinity II system (Santa Clara, US), equipped with a C18-column (Supelco C18 Discovery, 5 µm, 4.0 × 150 mm, Bellefonte, US) and a diode array detector (Agilent 1260 Infinity II DAD HS, Santa Clara, US) was operated isothermally at 30 °C and 50 °C for **2** and **3**, respectively. Measurements were run at a flow rate of 1.0 mL min^{-1}. For **2**, the mobile phase was water/methanol 55/45 (v/v) hold isocratically for 10 min and 1 µL sample was injected. For **3**, the mobile phase was water/methanol with a linear gradient of; t = 0 min, 55/45 (v/v); t = 4.0 min, 50/50 (v/v); t = 8.0 min, 42/58 (v/v); t = 11.50 min, 42/58 (v/v); t = 11.51 min, 55/45 (v/v); t = 13.00 min, 55/45 (v/v) and 4 µL sample was injected. Peak areas were measured by the integrator and transformed into concentration using the corresponding standard curves. For substrates **2** and **3**, the employed wavelength was 210 and 310 nm respectively, to detect the generated products.

HPLC-ESI-MS for confirmation. To confirm generation of the hydroxylated products **2a**, **3a** and **3b**, HPLC-ESI-MS was employed. An Agilent 6130 Quadrupole LC System (Santa Clara, US), was operated using an identical HPLC method and column as described in section 1.7, above. The ESI-MS was run using the following parameters: API-ES spray chamber with a drying gas flow of 12 L min^{-1}, nebulizer pressure of 50 psi, drying gas temperature 350 °C and a capillary voltage of 3500 V positive and negative. The mass detection for **2a**, **3a** and **3b** was performed in positive SIM-modus with m/z = 150 [M + H], 172 [M + H] and 190 [M + H], respectively.

Chiral HPLC-DAD. Chiral HPLC-DAD measurements for **1a** were performed according to Wissner and colleagues.[17] Chiral assessments of the products **2a** and **3a** were performed on an Agilent 1260 Infinity HPLC-DAD system (Santa Clara, US), equipped with a normal phase Chiralpak IC column (5 µm, 4.6 × 250 mm, Daicel, Osaka, JP), heated to 30 °C. Analysis was performed with a flow rate of 1.4 mL min^{-1} and 15 µL sample injection. For the separation of the **2a** enantiomers, n-hexane/isopropanol (95/5) was used as mobile phase and hold isocratically for 22 min. For the separation of **3a** enantiomers, n-hexane/isopropanol (90/10) was used and hold for 90 min.

Peaks were detected at 210 nm and 310 nm, respectively (Supplementary section 1, Figs. S5 and S12).

NMR for structural characterization and measurement of the optical rotation. The purity of the biosynthesized products was assessed by ^{1}H- and ^{13}C-NMR. Spectra were recorded on a Bruker Avance 500 spectrometer operating at 500.15 and 125.76 MHz, for ^{1}H- and ^{13}C-NMR, respectively. Spectra were recorded using DMSO-d6 for **2 a** and **3 b**, and $CDCl_3$ for **2 b** and **3 a** as solvent. The chemical shifts (δ) are reported in parts per million (ppm) relative to the standard tetramethylsilane (TMS, δ = 0). For identification of **3 a**, COSY-, HSQC- and HMBC-NMRs were performed. Optical rotations were determined using a Perkin Elmer 241 polarimeter at 589 nm and 22 °C.

(+)-(*R*)-1,2,3,4-Tetrahydroquinoline-4-ol 2 a (106 mg, yellow oil), biosynthesized with TDO variant F114H_A223T: $[\alpha]_D^{22} = +128$ (*c* 0.1, $CHCl_3$), chiral HPLC-DAD of raw product: 94% *ee*; chiral HPLC-DAD of pure product: 80% *ee* due to racemization during purification. ^{1}H-NMR NMR (DMSO-d6, 500.15 MHz) δ = 7.08 (d, 1 H), 6.91 (t, 1H), 6.46 (m, 2H), 5.76 (s, 1H), 4.96 (d, 1H), 4.53 (m, 1H), 3.23 (m, 1H), 3.12 (m, 1H), 1.69-1.82 (m, 2H) ppm. ^{13}C-NMR (DMSO-d6, 125.76 MHz) δ = 145.12, 129.34, 127.70, 123.28, 114.69, 113.40, 63.80, 36.18, 30.39 ppm. Results were in agreement with literature.[25,36]

Quinoline 2 b (20 mg, colorless oil), biosynthesized with TDO variant F366V: ^{1}H-NMR ($CDCl_3$, 500.15 MHz) δ = 8.92 (dd, 1 H), 8.13 (dd, 2 H), 7.81 (d, 1 H), 7.72 (ddd, 1 H), 7.54 (ddd, 1 H), 7.39 (dd, 1 H) ppm. ^{13}C-NMR ($CDCl_3$, 125.76 MHz) δ = 150.41, 148.30, 136.07, 129.47, 128.30, 127.80, 126.55, 121.08 ppm. Results were in agreement with literature.[37]

(+)-(1*S*,2*R*)-3-(Pyridin-2-yl)cyclohexa-3,5-diene-1,2-diol 3 a (114 mg, yellow oil) biosynthesized with TDO variant M220A_V309G: $[\alpha]_D^{22} = +169$ (*c* 0.1, MeOH), chiral HPLC-DAD: > 98% *ee*. ^{1}H-NMR ($CDCl_3$, 500.15 MHz) δ = 8.53 (d, 1H), 7.71 (dd, 1H), 7.63 (d, 1H), 7.19 (dd, 1H), 6.66 (d, 1H), 6.14-6.22 (m, 2H), 4.92 (d, 1H), 4.50 (m, 1H) ppm. ^{13}C-NMR ($CDCl_3$, 125.76 MHz) δ = 157.15, 148.01, 137.14, 136.12, 131.75, 124.69, 124.88, 122.16, 120.08, 69.04, 67.41 ppm. Results were in agreement with literature.[11]

2-Phenylpyridin-3-ol 3 b (6 mg, white solid) biosynthesized with TDO variant M220A_V309G: ^{1}H-NMR NMR (DMSO-d6, 500.15 MHz) δ = 10.14 (s, 1H), 8.17 (d, 1H), 8.01 (d, 2H), 7.44 (t, 2H), 7.35 (t, 2H), 7.21 (dd, 1H) ppm. ^{13}C-NMR (DMSO-d6, 125.76 MHz) δ = 151.48, 144.38, 140.19, 137.99, 128.79, 127.68, 123.49, 123.31 ppm. Results were in agreement with literature.[38]

Acknowledgements

This research was supported by the BMBF in the course of the project PowerCart 031B0369A. This research received funding from the European Union's Seventh Framework Programme for research, technological development and demonstration under grant agreement number 613849 in course of the project BIOOX. W. E.-H. thanks the Science and Technology Council of Mexico (Consejo Nacional de Ciencia y Tecnología, CONACYT) for financial support granted to work in this project. J. L. W. thanks Peter Heinemann for fruitful discussions and WesWizzArt and Wayra Castillo-Guerrero for the artistic contribution. Open Access funding enabled and organized by Projekt DEAL.

References

[1] M. A. Endoma, V. P. Bui, J. Hansen, T. Hudlicky, *Org. Process Res. Dev.* **2002**, *6*, 525–532.
[2] T. Hudlicky, *ACS Omega* **2018**, *3*, 17326–17340.
[3] D. R. Boyd, N. D. Sharma, C. J. McGivern, P. J. Stevenson, P. Hoering, C. C. R. Allen, *J. Org. Chem.* **2019**, *84*, 15165–15172.
[4] F. F. Özgen, S. Schmidt, *Biocatalysis* **2019**, 57–82.
[5] S. Resnick, K. Lee, D. Gibson, *J. Ind. Microbiol. Biotechnol.* **1996**, *17*, 438–457.
[6] D. R. Boyd, N. D. Sharma, S. A. Haughey, M. A. Kennedy, B. T. McMurray, G. N. Sheldrake, C. C. R. Allen, H. Dalton, K. Sproule, *J. Chem. Soc. Perkin Trans. 1* **1998**, 1929–1934.
[7] D. S. Torok, S. M. Resnick, J. M. Brand, D. L. Cruden, D. T. Gibson, *J. Bacteriol.* **1995**, *177*, 5799–5805.
[8] M. A. Vila, V. Steck, S. Rodriguez Giordano, I. Carrera, R. Fasan, *ChemBioChem* **2020**, *21*, 1981–1987.
[9] R. E. Parales, S. M. Resnick, *Biocatalysis in the Pharmaceutical and Biotechnology Industries*, CRC Press, **2006**, 299–331.
[10] M. A. Vila, M. Brovetto, D. Gamenara, P. Bracco, G. Zinola, G. Seoane, S. Rodríguez, I. Carrera, *J. Mol. Catal. B* **2013**, *96*, 14–20.
[11] D. R. Boyd, N. D. Sharma, G. P. Coen, F. Hempenstall, V. Ljubez, J. F. Malone, C. C. R. Allen, J. T. G. Hamilton, *Org. Biomol. Chem.* **2008**, *6*, 3957–3966.
[12] T. Sakamoto, J. M. Joern, A. Arisawa, F. H. Arnold, *Appl. Environ. Microbiol.* **2001**, *67*, 3882–3887.
[13] L. M. Newman, H. Garcia, T. Hudlicky, S. A. Selifonov, *Tetrahedron* **2004**, *60*, 729–734.
[14] N. Zhang, B. G. Stewart, J. C. Moore, R. L. Greasham, D. K. Robinson, B. C. Buckland, C. Lee, *Metab. Eng.* **2000**, *2*, 339–348.
[15] M. A. Vila, D. Umpiérrez, G. Seoane, S. Rodríguez, I. Carrera, N. Veiga, *J. Mol. Catal. B* **2016**, *133*, S410–S419.
[16] D. Boyd, N. Sharma, I. Brannigan, C. McGivern, P. Nockemann, P. Stevenson, C. McRoberts, P. Hoering, C. Allen, *Adv. Synth. Catal.* **2019**, *361*, 2526–2537.
[17] J. L. Wissner, W. Escobedo-Hinojosa, A. Vogel, B. Hauer, *J. Biotechnol.* **2021**, *326*, 37–39.
[18] M. A. Vila, D. Umpiérrez, N. Veiga, G. Seoane, I. Carrera, S. Rodríguez Giordano, *Adv. Synth. Catal.* **2017**, *359*, 2149–2157.
[19] R. Friemann, K. Lee, E. N. Brown, D. T. Gibson, H. Eklund, S. Ramaswamy, *Acta Crystallogr. Sect. D* **2009**, *65*, 24–33.
[20] B. Kauppi, K. Lee, E. Carredano, R. E. Parales, D. T. Gibson, H. Eklund, S. Ramaswamy, *Structure* **1998**, *6*, 571–586.

[21] M. Mohammadi, J. F. Viger, P. Kumar, D. Barriault, J. T. Bolin, M. Sylvestre, *J. Biol. Chem.* **2011**, *286*, 27612–27621.
[22] M. Nettekoven, J. Fingerle, U. Grether, S. Grüner, A. Kimbara, B. Püllmann, M. Rogers-Evans, S. Röver, F. Schuler, T. Schulz-Gasch, C. Ullmer, *Bioorg. Med. Chem. Lett.* **2013**, *23*, 1177–1181.
[23] M. Okamoto, O. Sakuragi, Y. Mori, M. Kishida, T. Higashijima, *Optically Active Cyclic Alcohol Compound*, **2013**, Patent No. US8471028B2.
[24] V. Sridharan, P. A. Suryavanshi, J. C. Menéndez, *Chem. Rev.* **2011**, *111*, 7157–7259.
[25] D. Zheng, M. Yang, J. Zhuo, K. Li, H. Zhang, J. Yang, B. Cui, Y. Chen, *J. Mol. Catal. B* **2014**, *110*, 87–91.
[26] D. R. Boyd, G. N. Sheldrake, *Nat. Prod. Rep.* **1998**, *15*, 309–324.
[27] S. Beil, J. R. Mason, K. N. Timmis, D. H. Pieper, *J. Bacteriol.* **1998**, *180*, 5520–5528.
[28] J. M. Halder, B. M. Nestl, B. Hauer, *ChemCatChem* **2018**, *10*, 178–182.
[29] C. Gally, B. M. Nestl, B. Hauer, *Angew. Chem. Int. Ed.* **2015**, *54*, 12952–12956; *Angew. Chem.* **2015**, *127*, 13144–13148.
[30] E. L. Ang, J. P. Obbard, H. Zhao, *FEBS J.* **2007**, *274*, 928–939.
[31] R. E. Parales, K. Lee, S. M. Resnick, H. Jiang, D. J. Lessner, D. T. Gibson, *J. Bacteriol.* **2000**, *182*, 1641–1649.
[32] R. E. Parales, S. M. Resnick, C. L. Yu, D. R. Boyd, N. D. Sharma, D. T. Gibson, *J. Bacteriol.* **2000**, *182*, 5495–5504.
[33] H. Suenaga, T. Watanabe, M. Sato, Ngadiman, K. Furukawa, *J. Bacteriol.* **2002**, *184*, 3682–3688.
[34] J. L. Wissner, J. Ludwig, W. Escobedo-Hinojosa, B. Hauer, *J. Biotechnol.* **2020**, *325*, 380–388.
[35] V. J. Kolcsár, F. Fülöp, G. Szőllősi, *ChemCatChem* **2019**, *11*, 2725–2731.
[36] C. Yin, X. Q. Dong, X. Zhang, *Adv. Synth. Catal.* **2018**, *360*, 4319–4324.
[37] Y. Fukazawa, A. E. Rubtsov, A. V. Malkov, *Eur. J. Org. Chem.* **2020**, *2020*, 3317–3319.
[38] W. X. Huang, B. Wu, X. Gao, M. W. Chen, B. Wang, Y. G. Zhou, *Org. Lett.* **2015**, *17*, 1640–1643.